A novel signal processing technique for separating tonal and broadband noise components from counter-rotating open-rotor acoustic data

Dave Sree
Professor, Mechanical Engineering Department, Tuskegee University, Tuskegee, AL 36088, USA
E-mail: dsree@mytu.tuskegee.edu

Renewed interest in counter-rotating open-rotor technology for aircraft propulsion application has prompted the development of advanced diagnostic tools to enable improved design and improved acoustical performance of open rotors. In particular, the determination of tonal and broadband components of open-rotor noise spectra is essential for properly assessing the noise control parameters and for validating noise prediction codes. Techniques that have been successfully used for processing acoustic data from single rotors (fans, propellers, etc.) do not work well for counter-rotating open-rotor systems in that the tonal and broadband noise components cannot be separated from raw acoustic data properly, particularly when the two rotors are driven independently without synchronization. The need for a new signal processing tool for counter-rotating open rotors was thus envisioned and is presented in this work. The new technique has been verified to perform well against simulated data as well as real acoustic data available from scale-model open-rotor tests at NASA-Glenn Research Center. Based on the results, the applicability and limitations of the technique are discussed in the paper.

1. INTRODUCTION

In this work, the term “open-rotor” refers to unducted counter-rotating twin rotors (propellers) which are being considered as propulsion devices for future aircraft [1, 2]. The open rotors are also known as ‘propfans’ or ‘unducted fans.’ Open-rotor propulsion technology is now being developed as a viable alternative to modern day turbofan engines mainly because of predicted fuel economy benefits and improved performance [3]. However, high noise levels associated with open rotors pose both environmental and technological challenges. These include community noise around airports, passenger discomfort, aircraft structural integrity, and meeting stringent federal noise regulations.

NASA-Glenn Research Center (GRC), in collaboration with the U. S. aircraft industry, is conducting both analytical and experimental research studies to address this noise issue and to develop improved open-rotor systems [4]. Extensive scale-model tests are being conducted in wind tunnels and in acoustic facilities to understand the noise mechanisms and to evaluate the acoustic performance of open rotors [5, 6]. Noise control measures may be targeted at one or more specific noise mechanisms. For example, the aft rotor diameter is kept smaller than the front one to try to limit the interaction with the tip vortices from the front rotor, which is a source of tonal noise. The tonal noise arises out of the mean wakes from rotor spin whereas the broadband noise is a result of complex unsteady aerodynamics around the rotors. The tonal noise could also be self-noise of each rotor.

These research studies have prompted development of advanced diagnostic tools capable of separating the tonal and broadband noise components from total open-rotor noise data. The characterization of tonal and broadband components is important for assessing critical noise control parameters and for validating noise prediction codes [7, 8]. At present, no data analysis tool is known by the author that can properly separate tonal and broadband components from measured open-rotor noise data, particularly when the two rotors are driven independently without synchronization and there is random phase change in the data record. Approximation of the broadband noise is sometimes made by "chopping off" the peaky tonal components of the overall noise spectra at their base and considering the remaining part as an estimate of the broadband noise [6, 9]. This procedure may be questionable and a basis needs to be established for it. Also, techniques that have been successfully used for processing acoustic data from single rotors (fan, propeller, etc.) do not work well for those from open-rotor systems in that the tonal and broadband noise components cannot be separated properly. This inability is attributed to complex flow structure around open rotors, jitter in rotor speeds, and other extraneous noise effects that cause random phase shifts to occur in the measured noise data [10]. These effects are not unique to open rotors but can happen with single rotors also. There was a need for the development of a proper data processing tool for open rotors. A new signal processing technique was thus envisioned.

The main purpose of this work is to present a new methodology for separating all rotor tones and broadband noise from counter-rotating propellers, particularly when the two rotors are driven independently without perfect synchronization. It is also to find out whether the new technique will provide a basis for verifying the practice of using the "chopping off" procedure to approximate broadband noise levels from overall noise spectrum and, in addition, to see if it can be helpful in identifying the interaction of unwanted noise in corrupted open-rotor experimental data.

The methodology of the new technique along with selected results from simulated data and real scale-model open-rotor test data, to validate its applicability and limitations, are presented in this paper. A brief description of the single rotor technique and a discussion of why it does not work for open rotors will be given before presenting the new technique.

2. SINGLE ROTOR TECHNIQUE

In the single rotor technique, first, a phase-averaged mean over one full rotation of the shaft (i.e. over a given number of rotor blade passages) is computed. (Phase averaging is performed to separate the periodic and the fluctuating components in the test data from rotating systems. The periodic component could be steady or time-varying). This is done by sorting all the measured unsteady pressure data according to the "rev" (revolution) markers in once-per-revolution ("1/rev") data, overlaying them in one shaft rotation time window, and taking an ensemble average of the overlaid data. This ensemble average is usually periodic and is known as the "phase-averaged mean." It represents the "tonal" component of the total noise. (The measured "raw" data will be referred to as the "overall" signal here onwards). The phase-averaged mean obtained this way is then properly subtracted from the overall signal to obtain the "broadband" component. (It should be noted here that the same phase-averaged mean, computed only once, is being repeatedly used to determine the broadband component). Once the tonal and broadband components are separated, an FFT (Fast Fourier Transform) operation with a suitable smoothing window is applied on each component to obtain the corresponding noise spectra. A number of data blocks are used to average and arrive at the final results. This technique works well for data obtained from single rotor systems but not for those from open rotors. The following example explains this situation.

2.1. APPLICATION OF SINGLE ROTOR TECHNIQUE TO OPEN-ROTOR DATA

The noise data required for this example were generated using a scale-model open-rotor system arranged in a "pusher" configuration. This system, called the "mini open-rotor," is as shown in Figure 1. The purpose of the mini open-rotor apparatus was to have a test bed for developing acoustic measurement methodologies in a repeatable, inexpensive, flexible, and high signal-to-noise environment. This non-proprietary test bed also enables verification of acoustic measurement techniques prior to entry into a more expensive and less available environment [11]. This model was tested in the Applied Aeroacoustics Propulsion Laboratory [12] at NASA-GRC where the background noise was considered to be low (below 40 dB).

The mini open-rotor system was about 22.9 cm (9 inches) in diameter and had 4 forward and 3 aft blades. The two counter-rotating rotors were driven independently. Their speeds were monitored by two separate fiber optic sensors (tachometers) by recording the "1/rev" data. The two rotors could be arranged to run at equal or unequal speeds. At equal speeds, they were not perfectly synchronized. Microphones were set up on either side of the model to measure the noise at different sideline locations. The results presented in the example here are for data obtained at an azimuthal sideline location of 152.4 cm (5 ft) from the model on the port side when both rotors were running approximately at 6757 RPM. The unsteady pressure (acoustic) data along with the forward and aft "1/rev" signals were simultaneously collected on the facility data system using a sampling frequency of 50 kHz. A 2 Hz–10 kHz band-pass filter was used to cut off unwanted noise. At least 100 blocks of data were used to perform the FFT analysis with a frequency resolution of 12.2 Hz.

Figure 2 shows the overall, tonal, and broadband spectral results obtained using the single rotor technique on the mini open-rotor acoustic data. The spectral values are plotted as SPL (sound pressure level),

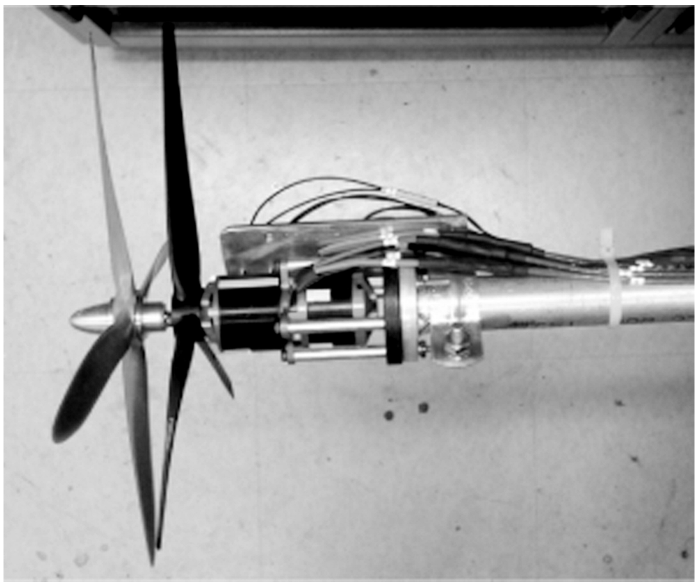

Figure 1: Photograph of mini-open rotor model.

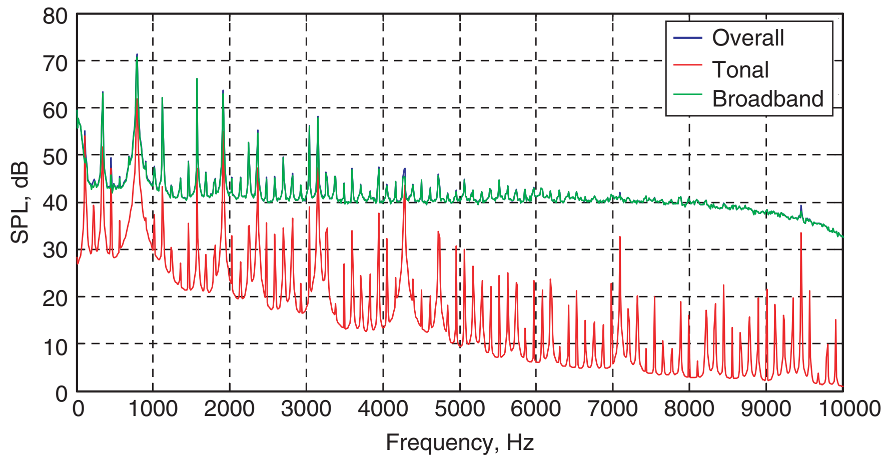

Figure 2: Overall, tonal, and broadband spectra obtained using single rotor technique (SPL vs Frequency).

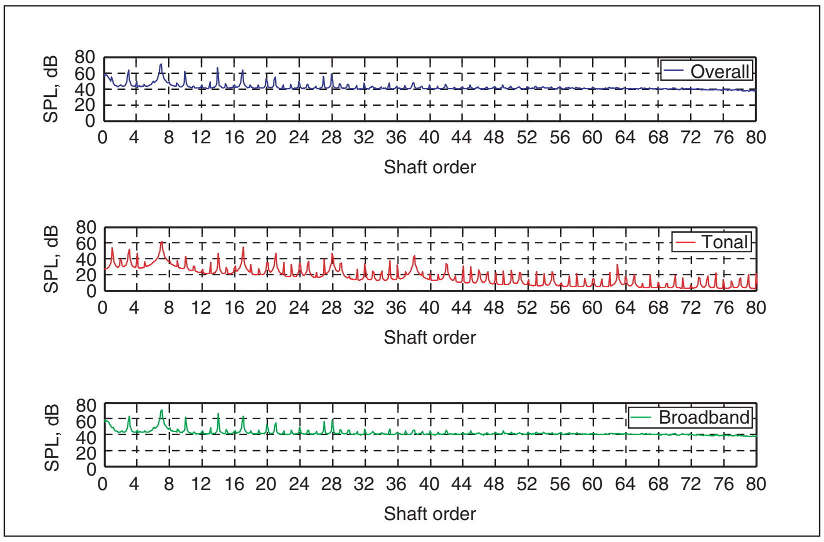

Figure 3: Overall, tonal, and broadband spectra obtained using single rotor technique (SPL vs Shaft-order).

in dB (reference pressure = 20 × 10^{-6} Pa), versus frequency, in Hz. The spectra are overlaid to show the relative differences in SPL. The same results are shown again in Figure 3 where the individual spectra are plotted separately for clarity, this time showing SPL versus shaft-order instead of frequency. (Shaft-order = Frequency/RPS, where RPS = revolutions per second). As seen from the plots in Figures 2 and 3, it is clear that the tonal and broadband components are not cleanly separated because the broadband component (green), which is supposed to be free of tone noise, still shows strong "tone" like spikes in it. These spikes are comparable to tonal noise (red). They are as much as the overall (blue) noise itself. This indicates that the single rotor technique cannot separate the tonal and the broadband components from total open-rotor noise properly. It does not work well for open-rotor data.

The failure of single rotor technique for open rotors is attributed to the jitter or deviations in rotor speeds and/or other extraneous noise effects which cause random phase shifts in the measured data. These phase shifts result in distorting the phase-averaged mean which is determined by ensemble averaging of all the measured overall signals over one full shaft rotation. There is no easy fix for this, particularly with open-rotor data. As shown in Figure 4, the ensemble or overlay of all the measured overall signals (blue) over one shaft rotation becomes fuzzy. It does not lead to a well-defined "periodic" pattern of the phase-averaged mean that is commonly seen from good single rotor records. This is revealed by the red curve in Figure 4. Thus, the presumed correct identity of the phase-averaged mean for open-rotor data is lost in the ensemble averaging process which further leads to incorrect determination of the broadband component. The putative broadband signal becomes partially periodic (see Figure 5) showing strong "tone" like characteristics in the broadband noise spectrum (see in Figure 2 or 3). These phase change effects are not unique to open rotors but can happen with single rotors also. Thus, a new technique was required to process open-rotor data.

3. THE NEW TECHNIQUE

In the new technique, the raw data set is first arranged into small uniform segments. The segment length or size selected depends on the desired frequency resolution in the FFT analysis. If the segment length, in terms of number of sampled data points, is NFFT, then the frequency resolution, Δf, is given by: $\Delta f = f_s / NFFT$ where f_s, is the sampling frequency. The spectral values obtained through FFT then will be from zero to the Nyquist frequency, $f_s/2$.

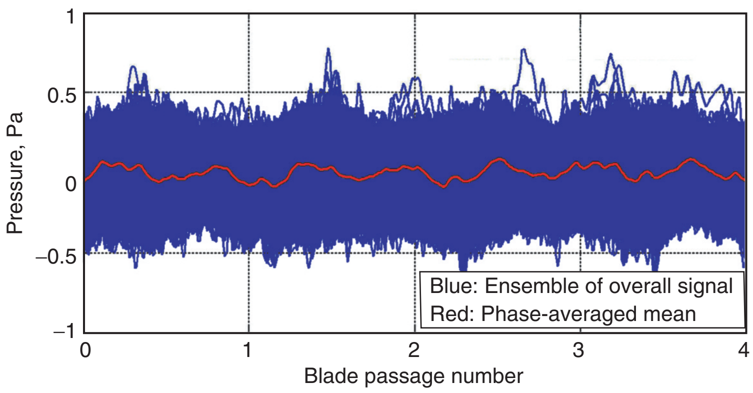

Figure 4: Phase-averaged mean obtained using forward rotor "1/rev" signal and single rotor technique.

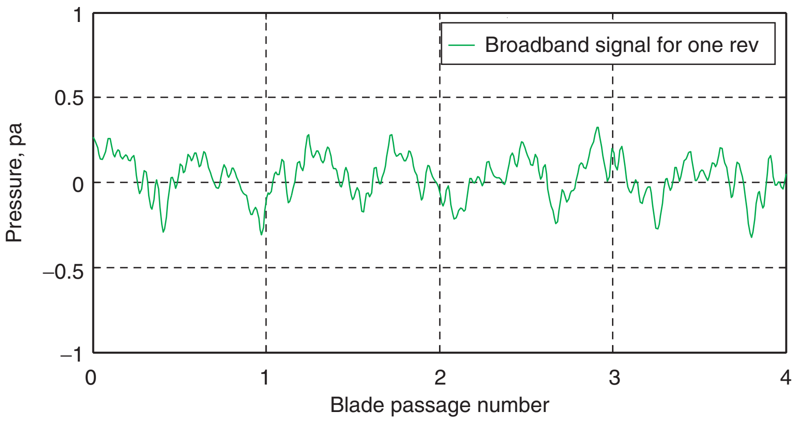

Figure 5: Sample broadband signal for one revolution obtained using forward rotor "1/rev" signal and single rotor technique.

Segments can be selected in several ways. From the author's experience, it is better that the segments selected always begin from a given reference point in the data record. The "1/rev" signal comes in very handy for this purpose. For example, if the first segment begins from a "rev" marker in the "1/rev" data and lasts for, say, 8.5 revolutions of data, then the second (subsequent) segment should begin from a similar marker on the 9th revolution and should last for 8.5 revolutions from there, and so on. Overlap of the same data points should be avoided.

As mentioned before, jitter in shaft rotations and other extraneous effects cause phase shifts to occur in the measured open-rotor acoustic data. These phase shifts, if any, can be easily detected by inspecting a plot of the number of data points occurring in each revolution (N/rev) versus the "rev" number. The "N/rev" information is obtained by counting the data points between the appropriate "rev" markers in the "1/rev" record. For this purpose, either the forward or the aft rotor "1/rev" record can be used. With continuous sampling during data collection, the "N/rev" value varies from revolution to revolution because of the drift in shaft speed. An example of such a plot generated from the mini open-rotor data is shown in Figure 6. The shape of this kind of plot, in realty, can be different depending on the nature of phase shifts. It is noted from this figure that the "N/rev" is not the same in every revolution. It varies from revolution to revolution causing phase shifts to occur in the data record.

The phase shifts, as discussed earlier, cause the tonal component to become distorted if the ensemble averaging process were to be used. The distortion of the tonal component can be avoided if a fewer number of data segments are considered to compute it. The idea is to capture distinctly the "best" shape of the mean of the segments, before it gets distorted [10]. A minimum of two segments is required for this purpose. The mean computed from just two segments will be termed as the "segment-averaged mean" here. It is a point-wise averaging of the data in the two segments and is similar to phase-averaging in single rotor technique.

But, before computing the segment-averaged mean, a cross-correlation operation is performed to determine the amount of dominant phase shift between the two segments under consideration based on the maximum cross-correlation value. The two segments are then lined up properly to account for this phase shift. This will minimize the distortion of the computed segment-averaged mean, i.e. the tonal component. This is the approach taken in the new technique to determine the tonal component from

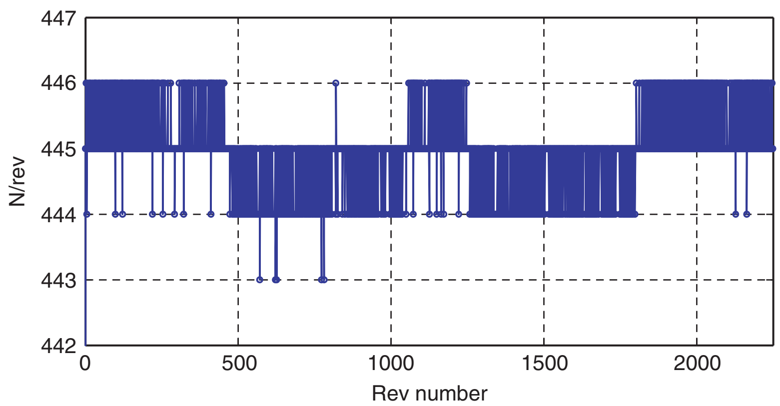

Figure 6: A plot of number of points per revolution (N/rev) vs "rev" number obtained using forward rotor "1/rev" signal.

the overall signal at each step. The tonal component is subtracted from the overall signal to determine the broadband component in each segment. FFT and other statistical operations are then performed to obtain the desired results for a pair of segments or, as it will be called, a "block" of data. This way, starting from the beginning of the data record, the process is continued until all the "blocks" in the whole record are taken into account. In the end, a proper averaging is performed to obtain the final results.

The technique described so far can also be used for processing single rotor data. The main difference between this technique and single rotor technique is that, unlike in the single rotor technique where only one phase-averaged mean is used for the entire data set, separate segment-averaged means are computed for each "block" of data in the new technique.

The steps involved in the new data processing technique are listed as follows:

1. Based on the frequency resolution (Δf) desired, select a segment size (NFFT) for the FFT operation of the raw data. (Follow the suggested procedure for data segment selection).
2. Take two such consecutive segments (say, x and y) from the beginning of the raw data set, perform cross-correlation operation, and determine the dominant phase shift ($\Delta\tau$) between them based on maximum cross-correlation value. (x and y data will be called the "overall" signals and they represent the total noise).
3. Depending upon the "lag" or "lead" in phase shift, skip by amount (or equivalent number of bins) and redefine the beginning of one of the segments that is to be "phase-adjusted." Note that some data padding from neighboring segment may be required to keep its length as NFFT to match with the other segment. (For sake of convenience here, the same nomenclature x and y will be maintained for the phase-adjusted segments).
4. Then, determine the segment-averaged mean (say, z) for the two segments after phase adjustment. Note that this mean is common to both segments. "z" data represents the "tonal" part of the total noise.
5. Next, determine the fluctuating components (say, x' and y') of the data in the two segments using: $x' = x - z$ and $y' = y - z$. These x' and y' data represent the "broadband" part of the total noise.
6. After separating these components, perform FFT and other statistical operations on x, y, z, x', and y' data using any available software, such as MATALB. Obtain the overall, tonal, and broadband power spectra and statistical parameters of interest. The average of the spectral and statistical results for x and y data is taken as the desired result for the "overall" component for one block of data. (Note: The two segments together represent one block). A similar average from x' and y' data gives the desired result for the "broadband" component for the same block. The computed result from z data is the result for the "tonal" component of that block. Thus, steps 2 to 6 give the required results for just one block of data.
7. Next, take another pair of similar segments, subsequent to the first two segments, from the raw data and repeat the process from steps 2 to 6 and get the results for the second block. In a similar way, move on to the next set of segments, repeat steps 2 to 6. Accumulate the individual block results until all the "nblks" in the data set are finished. (Since two segments together define one block, the total number of blocks available in the entire data set is given by:

nblks = [total samples in the data set /(2*NFFT)] – 1

where "−1" indicates reserving some samples for data padding, if any, at the end).

8. In the end, compute a final average over "nblks" for all the desired outputs (overall, tonal, and broadband spectra, etc.) for the data set selected and plot as required.

4. APPLICATION OF THE NEW TECHNIQUE

The applicability and limitations of the new technique are investigated using examples of simulated data as well as real data from a scale-model open-rotor acoustic test. Examples of simulated data are considered first.

4.1. SIMULATED DATA

Four examples of simulated data are considered as follows:

(i)A sine wave to simulate pure tone,

(ii)White noise to simulate pure broadband noise,

(iii)A sine wave with white noise to simulate tonal and broadband noise, and

(iv)Multiple sine waves with white noise to simulate multiple tones and broadband noise.

In each example, a sampling frequency of 1000 Hz was used to obtain the digitized data and a segment size of 1000 data points or samples was selected to give a 1-Hz frequency resolution in the spectral analysis. The amplitude of each sine wave was set to 1.0. Normally-distributed pseudo-random numbers, with mean 0.0 and variance 1.0, were generated in the last three cases to simulate white noise. A variety of phase shifts between the data segments was introduced in all the four cases. Hanning window was used to smooth the spectral estimates. Error calculations of the spectral estimates were based on the exact variance of the input data and the computed variance from each spectrum. In the new technique, 2 raw data segments amount to 1 block of data. Based on error calculations, for examples involving white noise, at least 25 blocks of data (i.e. more than 50,000 samples, the more the better) were required to obtain the final spectral results within ±1.0% statistical accuracy. Pure sine wave examples require significantly less number of data blocks to achieve that accuracy. All the computations were performed using MATLAB software.

4.1.1. Pure sine wave

A 10-Hz sine wave of amplitude 1.0 was considered here. In order to illustrate the methodology of the new technique, only 1 block of data was used in this example. How the segment-averaged mean can get distorted is also illustrated in this example. The two segments of the digitized data, say, x (blue) and y (red), are shown in Figure 7 and they have a phase-shift $\Delta\tau$ (0.02 s) between them. If one were to compute the "phase-" or segment-averaged mean of x and y, it would yield the black curve z as the segment mean, which we know is not the desired mean. Then, subtraction of this mean from the two sine waves would result in the respective broadband components, x' (magenta) and y' (cyan), as shown in Figure 8. FFT operation on these signals would yield the spectral results as shown in Figure 9 which we realize are not the correct results we are looking for. But, as we know, without phase shift between x and y, the segment-averaged mean should also be sine wave of amplitude 1.0 having a variance (or power) of 0.5 and each broadband component should have value zero. The wrong results are because of the phase shift that exists between the two segments. Now, if cross-correlation operation is applied on x and y, the dominant phase shift between them, based on the maximum cross-correlation (C_{xy}) value (see Figure 10), can be determined to be $\Delta\tau = 0.02$ s. If this phase shift is properly applied back to line up x and y, the segment-

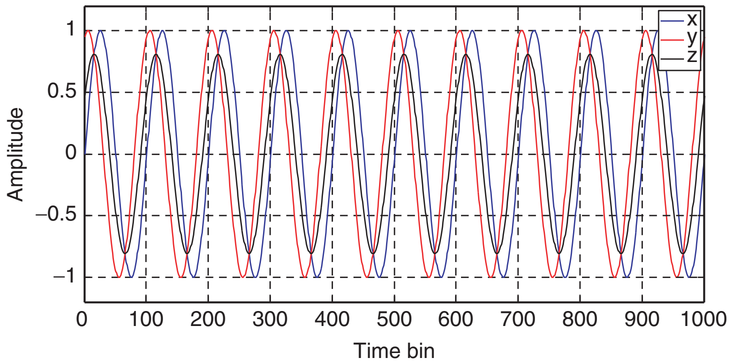

Figure 7: *Example of two sine wave segments (x and y) that are phase-shifted and the corresponding segment-averaged mean (z).*

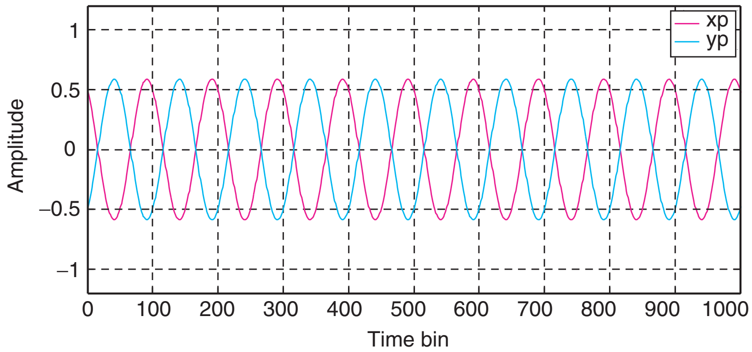

Figure 8: *Broadband signals (shown as xp and yp instead of x′ and y′) obtained from phase-shifted sine wave segments in Figure 7.*

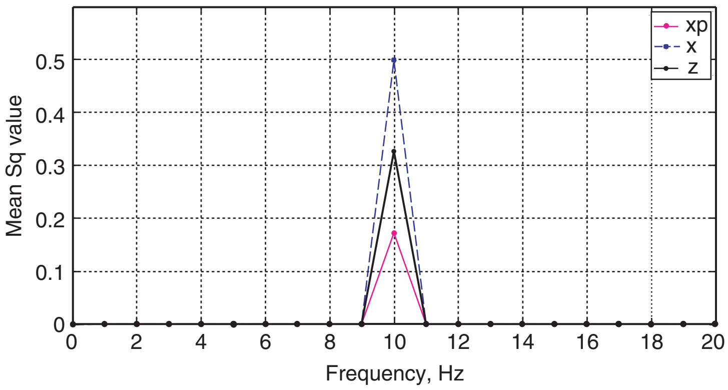

Figure 9: *Power spectra of sine wave segment, segment-averaged mean, and the corresponding broadband signal before phase-adjustment.*

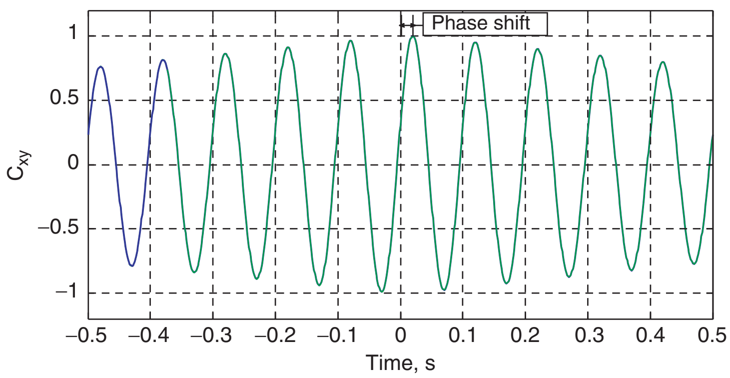

Figure 10: *Cross-correlation plot of sine wave segments showing the phase-shift at maximum cross-correlation value.*

averaged mean would become a sine wave of amplitude 1.0 as shown by the black curve in Figure 11 and the broadband components would become zero which we know are the correct answers. FFT operation on the tonal and broadband components then would yield the correct spectral results, as shown in Figure 12. This is confirmed by the computed variances of each component in the final results. The spectral estimates in this example were obtained within ±0.1% accuracy.

4.1.2. White noise

As stated earlier, white noise simulates pure broadband noise in the signal. Data required for this example were obtained by generating normally-distributed pseudo-random numbers with mean 0.0 and variance 1.0. The final spectral results (in dB) from the new technique are shown in Figure 13. (In this and the next two examples of simulated data, a reference value of 5×10^{-3} was used to convert the spectral values to dB). The results show that the total or "overall" noise (blue) is split equally between "tonal" (red) and "broadband" noise (green). As can be seen, there is a –3 dB difference between the "overall" and the "broadband" spectra. This is confirmed by computing the energy content or variance of each signal from the respective power spectrum. The

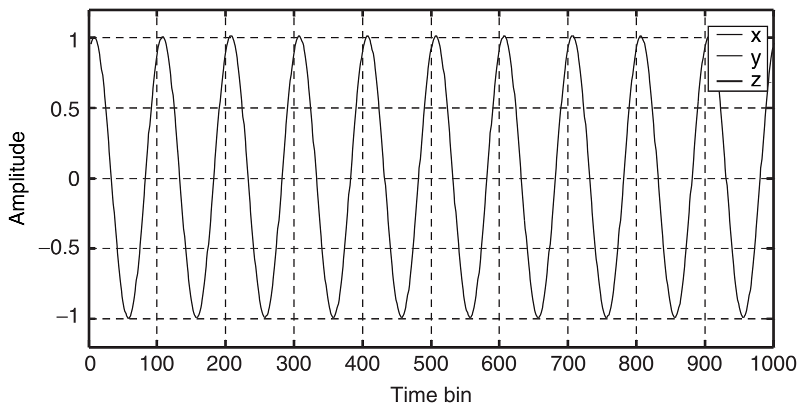

Figure 11: Segment-averaged mean after phase-adjustment (x and y segments after phase adjustment hiding behind z).

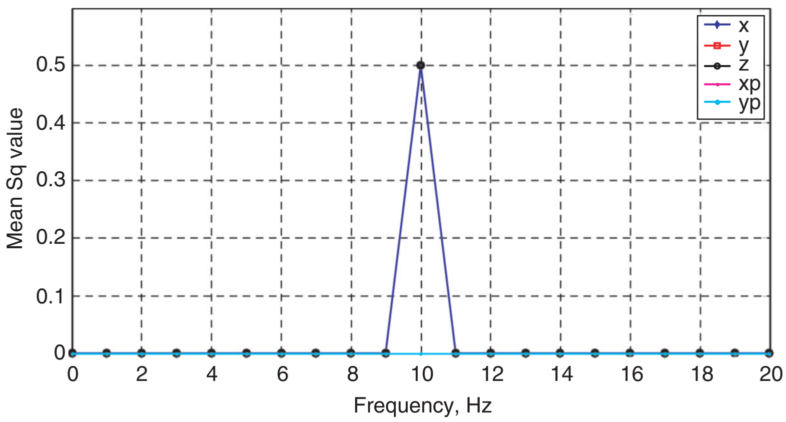

Figure 12: Power spectra of sine wave segments, segment-averaged mean, and the corresponding broadband signals after phase-adjustment (x and y spectra hiding behind z spectrum, and xp spectrum behind yp spectrum at bottom).

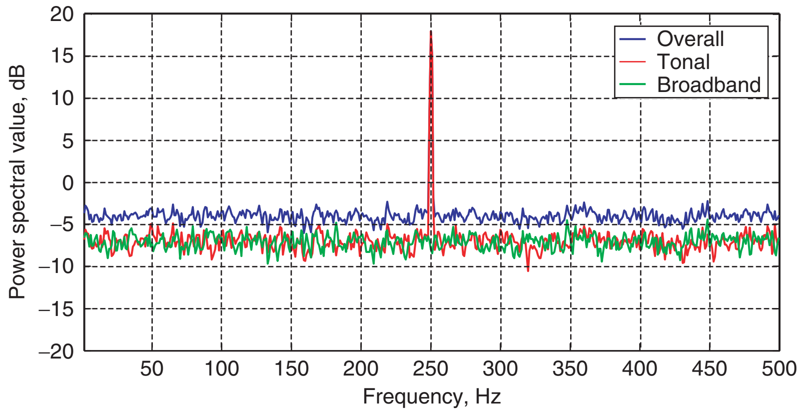

Figure 13: Overall, tonal, and broadband spectra of pure white noise, obtained using new technique.

variance of the "overall" signal is computed to be very close to 1.0 which we know is the correct answer. The computed variance of the "tonal" part is found to be about 0.5 and that of the "broadband" part is also about 0.5. Since we know that there is no tone present in the white noise here, the "flat" broadband spectral values (before converting them to dB) must add up to 1.0 to match with the total energy content in the signal. The "tonal" part in this example must be ignored. Therefore, before converting to dB, the broadband spectral values determined from the new technique will have to be multiplied by 2 to get the correct broadband noise levels.

4.1.3. A sine wave with white noise

In this example, a 250-Hz sine wave of amplitude 1.0 is mixed with white noise to simulate a single tone and broadband noise in the acoustic signal. Different phase values were introduced between the segments to check the validity of the new technique. The final spectral results (in dB) for this example are shown in Figure 14. The "overall" power spectrum (blue), showing a peak or the "tone" at 250 Hz, is correctly obtained. The computed variance from this spectrum is 1.5 (0.5 from sine wave + 1.0 from white noise), as expected. Again, as in the previous example, the white noise part of the "overall" spectrum is split equally between "tonal" (red) and "broadband" (green) spectra. This is confirmed by computing the energy content or variance of each signal from the respective spectrum. The variance computed from broadband spectrum is 0.5 which we know should be really close to 1.0 because the white noise added to pure tone has variance of 1.0. Therefore, the broadband spectral values, before converting them to dB, must be multiplied by 2 to obtain the correct broadband noise levels from the new technique. Then, the "tone only" spectral values, before converting them to dB, will be found by systematically subtracting the "corrected" broadband spectral values from the "overall" spectral values.

4.1.4. Multiple sine waves with white noise

This example is very similar to the one just discussed above except that multiple (two, three, and four) sine waves mixed with white noise were studied. Each case simulates multiple tones and broadband noise present in the "overall" signal. A variety of phase shifts, involving different combinations, were introduced to check the validity of the new spectral technique. The new technique worked well in each case. The results for the case involving four sine waves (each of amplitude 1.0) mixed with white noise are only presented and discussed here.

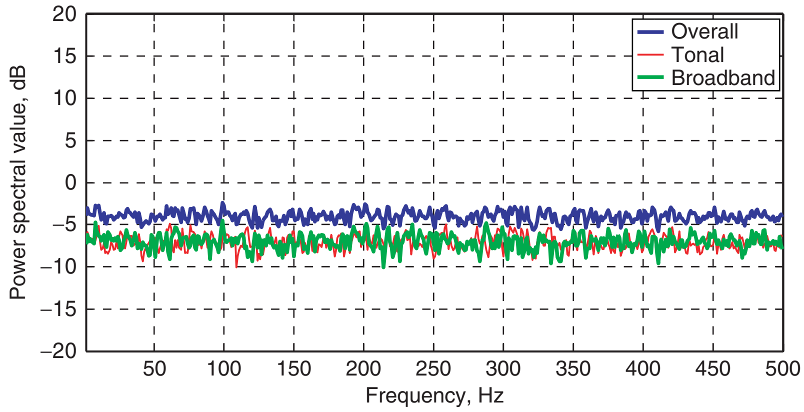

Figure 14: Overall, tonal, and broadband spectra of sine wave mixed with white noise, obtained using new technique.

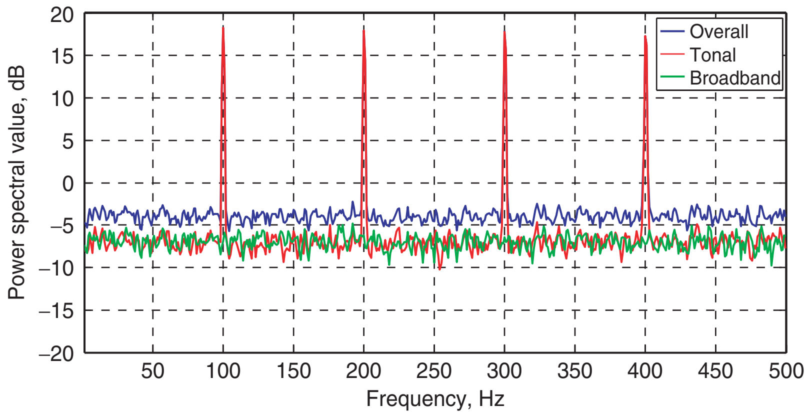

Figure 15: Overall, tonal, and broadband spectra of multiple (four) sine waves mixed with white noise, obtained using new technique.

The frequencies selected were 100 Hz, 200 Hz, 300 Hz, and 400 Hz.

The final spectral results (in dB) for this example are shown in Figure 15. The "overall" power spectrum (blue), showing the "tones" at 100 Hz, 200 Hz, 300 Hz, and 400 Hz, is correctly obtained. As expected, the computed variance from this spectrum is 3.0 (0.5 from each sine wave + 1.0 from white noise). Again, as in the previous example, the white noise part of the "overall" spectrum is split equally between "tonal" (red) and "broadband" (green) spectra. This is confirmed by computing the energy content or variance of each signal from the respective spectrum. The variance computed from broadband spectrum is again 0.5 which we know should be really close to 1.0 because the white noise added has variance of 1.0. This example also confirms that the broadband spectral values, before converting them to dB, must be doubled to obtain the correct broadband noise levels from the new technique.

Figure 16 shows a plot of the overall and the "corrected" broadband spectra for this case. It is noticed that the broadband spectrum (green) matches reasonably well with the "flat" portion of the overall spectrum. This is true in example (iii) also. Thus, the new technique provides a basis to validate the "chopping off" procedure to obtain the broadband spectrum from overall spectrum. As explained before, the "tone only" spectral values can be found by subtracting the "corrected" broadband spectral values from the "overall" spectral values.

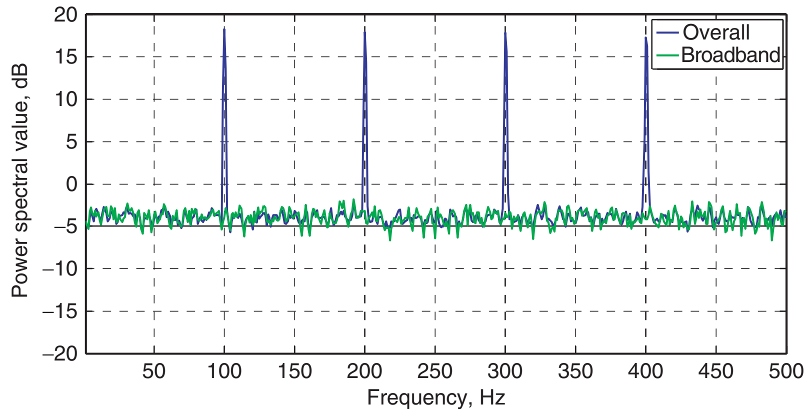

Figure 16: Tonal and "corrected" broadband spectra of multiple (four) sine waves mixed with white noise, obtained using new technique.

4.2. REAL DATA

The mini open-rotor data used in the example of single rotor technique (see Section 2.1) will be utilized here also to highlight the applicability of the new technique to real data. It may be recalled that this far-field acoustic data, along with the "1/rev" signals, were sampled at 50 kHz using a 2 Hz–10 kHz band-pass filter. The two rotors were driven independently. The speeds were very nearly the same and they were not perfectly synchronized. A segment size of 4096 samples was chosen to give a frequency resolution of 12.2 Hz. At least 100 blocks of data were used to average the spectral results.

Cross-correlation was applied at each stage to determine the dominant phase shift before the segment-averaged mean was calculated. A sample plot of two segments of overall signal (blue) and the corresponding segment-averaged mean (red) after phase-adjustment is shown in the top plot of Figure 17. One of two broadband components, after subtracting the segment-averaged mean from the overall signal, is shown in green in the bottom plot.

Figure 18 shows the final spectral results for the overall, tonal, and broadband components obtained from the new technique. These results are plotted together to show the relative SPLs (in dB, referenced to 20×10^{-6} Pa) as a function of frequency. The same overall and "corrected" broadband spectral results are plotted as SPL versus shaft-order in Figure 19. It is noticed in this figure that the "flat" part of the broadband spectrum (green) matches fairly well with the "flat" portion of the overall spectrum. Hence, it is reasonable to assume that these results support the "chopping off" procedure of obtaining the broadband spectrum from overall spectrum. Thus, the tonal and the broadband components have been resolved successfully using the new technique.

It Figure 18 or 19, the tone noise from aft rotor at shaft-order 3 (about 338 Hz) and the interaction tonal noise at shaft-orders 7, 10, 14, etc. can be easily noticed. The broadband spectrum shows some "tone" like spikes which may be real or could be due to interaction of the background noise with open-rotor noise. The background noise measured at three different times during the test was found to be around 38 dB, about 2–3 dB below the broadband noise level, as shown in Figure 20. The noise interaction is noticeable particularly at low frequencies (below 200 Hz or shaft-order less than 2) and around shaft-order 38 (about 4,280 Hz). Thus, the new technique can be helpful in identifying unwanted noise in experimental data.

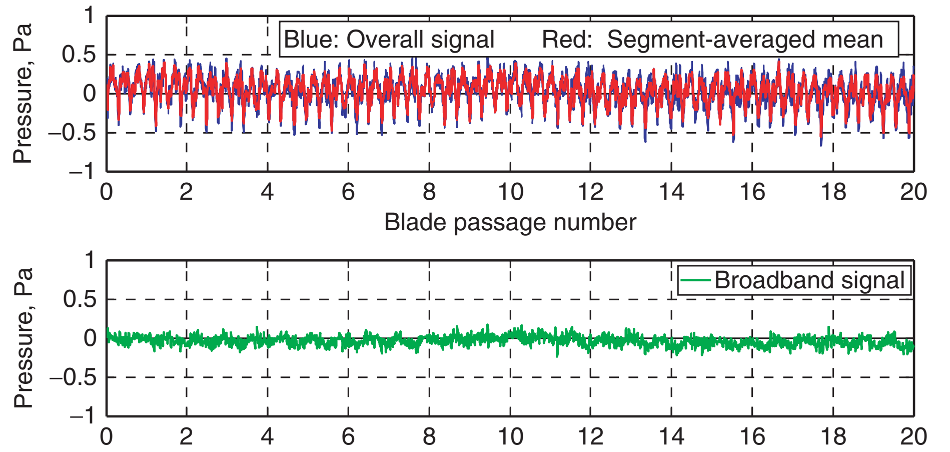

Figure 17: *Sample plots of overall signal and segment-averaged mean (top) and the corresponding broadband signal (bottom) after phase-adjustment, obtained using new technique.*

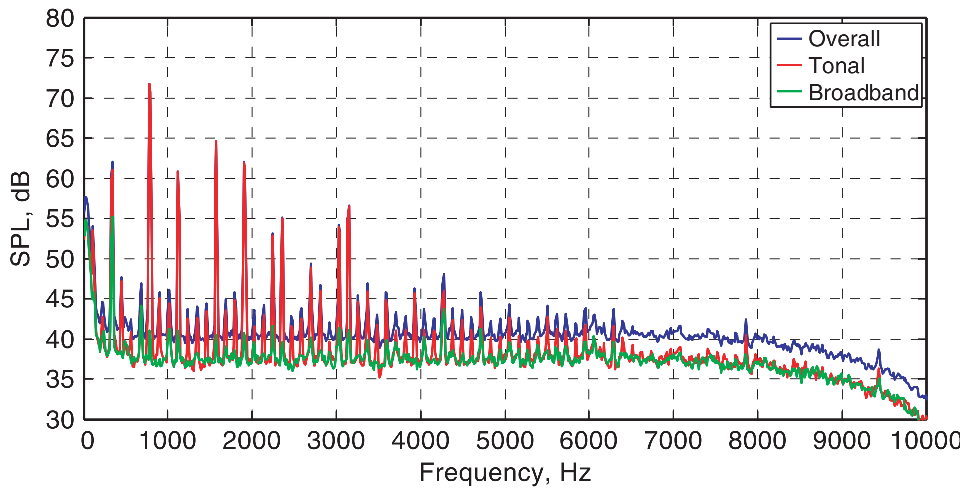

Figure 18: *Overall, tonal, and broadband spectra obtained using new technique (SPL vs Frequency).*

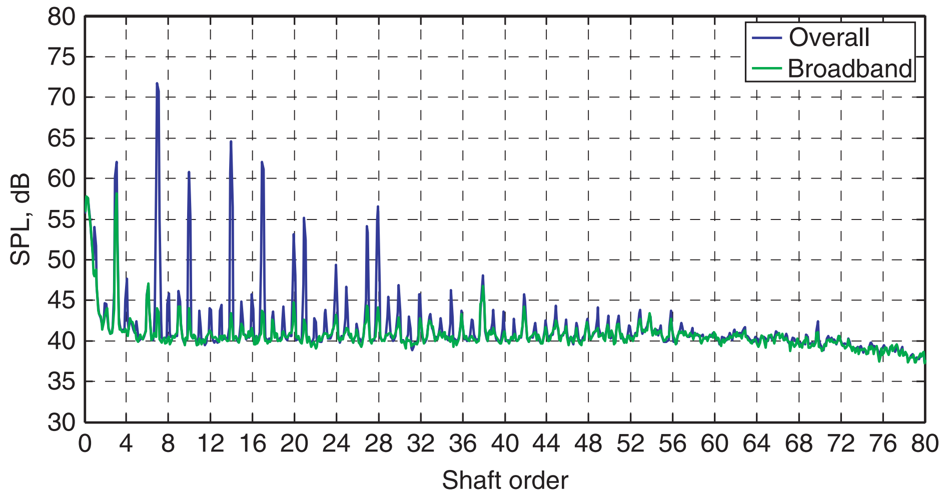

Figure 19: *Overall and "corrected" broadband spectra obtained using new technique (SPL vs Shaft-order).*

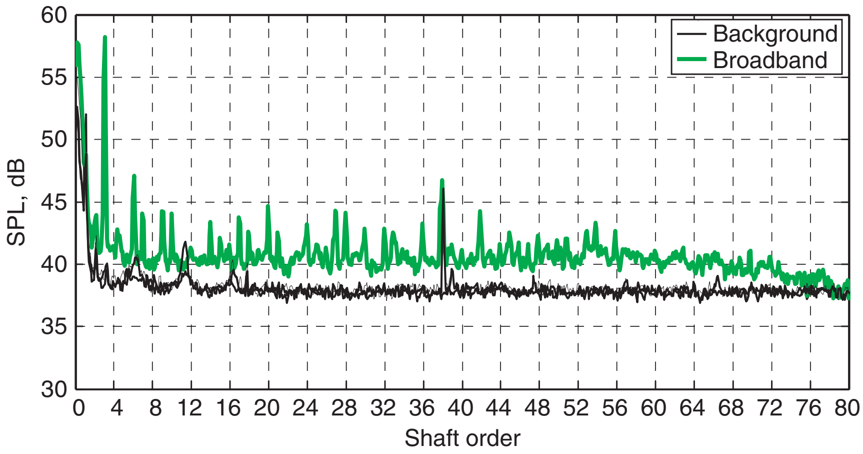

Figure 20: Comparison of "corrected" broadband noise with background noise.

The high spike of the broadband noise at shaft-order 3 may be attributed to the periodicity of strong wakes from the front rotor impinging on the aft rotor and getting locked on to the rotor blades, i.e. tonal and broadband noise may be coupled. They may be influencing each other and, hence, are not entirely separable. The other aspect, as we learnt earlier, is that some phase shifts, that were not accounted for by the new technique also cause spikes to appear in the broadband spectrum. It corrects for the most dominant phase shift only. These facts indicate limitations of the new technique. However, on an overall basis, these broadband spikes are significantly smaller than their corresponding tonal noise components. Thus, the results presented here demonstrate that the new technique works reasonably well in separating the tonal and the broadband components from total open-rotor noise.

It was verified in this research work that the new technique provides almost exactly the same results whether the data segment selection is made with respect to forward rotor or aft rotor "1/rev" signal, particularly when the two rotor speeds are about the same. Preliminary studies show that it works well when the speeds are unequal also. The new technique has also been verified to perform well against data from another open-rotor model having three times more number of blades. Those results will be published elsewhere.

5. CONCLUSIONS

Unique signal processing tools are required to understand the acoustic characteristics of counter-rotating open-rotor propellers. A novel approach to separate the tonal and broadband components of open-rotor noise has been presented in this work, particularly when the two rotors are driven independently without synchronization. The methodology of the new technique has been described in detail. The applicability and limitations of the technique have been validated using simulated data and real data from scale-model open-rotor systems. The technique works reasonably well regardless of whether the data samples are sorted with reference to forward rotor or aft rotor "1/rev" signal. The broadband spectral results obtained from this technique must be doubled to get the correct broadband noise levels (-this is assuming the broadband is of white noise type). The new technique provides a basis for validating the "chopping off" procedure to obtain broadband noise levels from overall spectrum. It also can be helpful in identifying unwanted noise in experimental data.

The "1/rev" signal helps to detect the presence of any phase shift in the noise data record. The new technique corrects only for the most dominant phase shift. Random phase shifts due to drift in rotor speeds, extraneous noise interactions, and/or strong coupling between tonal and broadband noise, do hinder or limit efficient separation of the broadband component from total noise with the new technique.

The new technique has been shown to perform well when the two rotor speeds are approximately equal. Preliminary study shows that the new technique works well when they are unequal also, but more investigation is required.

Lastly, the new technique presented here can be also used for processing acoustic or flow data from single rotor systems.

ACKNOWLEDGEMENTS

This work was performed under the 2010 Summer NASA-GRC Faculty Fellowship Program (NGFFP). The support from the University Affairs Office and the Acoustics Branch at NASA-GRC is greatly appreciated. In particular, the author expresses his sincere thanks to Dr. Daniel L. Sutliff of the Acoustics Branch for providing a photograph of the mini counter-rotating open-rotor model and the data necessary to do this work. Without his encouragement and fruitful discussions this research would not have been possible. The author would also like to thank Dr. David B. Stephens of the Acoustics Branch for his interest and helpful suggestions in this work.

REFERENCES

1. Building a Better Plane, NASA News & Features, May 3, 2010, *http://www.nasa.gov/topics/aeronautics/features/openrotor_prt.htm*

2. James, T., Back to Propellers, *Engineering and Technology Magazine*, 4 (10), 2 June 2009, *http://eandt.theiet.org/magazine/2009/10/back-to-propellers.cfm*

3. Fuel prices drive new look at open rotor jet engines, *Engineering and Technology* Magazine, 27 October 2008, http://eandt.theiet.org/news/2008/oct/open-rotor-test.cfm

4. GE and NASA Partner on Open Rotor Engine Testing, NASA-Ask the Academy, 2 (3), 30 March 2009, http://www.nasa.gov/offices/oce/appel/ask-academy/issues/ volume2/AA_2 3_F_ge_rotor.html

5. Elliott, D. M., Initial Investigation of the Acoustics of a Counter Rotating Open Rotor Model with Historical Baseline Blades in a Low Speed Wind Tunnel, in: *Proceedings of the 17th AIAA/CEAS Aeroacoustics Conference (32nd AIAA Aeroacoustics Conference*), Portland, OR, 05–08 June 2011.

6. Stephens, D. B., Nearfield Unsteady Pressure at Cruise Mach Numbers for a Model Scale Counter-Rotation Open Rotor, in: *Proceedings of the 18th AIAA/ CEAS Aeroacoustics Conference (33rd AIAA Aeroacoustics Conference*), Colorado Springs, CO, pp. 04–06 June 2012.

7. Magliozzi, B., Hanson, D. B. and Amiet, R. K., Propeller and Propfan Noise, Chapter 1, *Aeroacoustics of Flight Vehicles: Theory and Practice, Volume 1*: Noise Sources, NASA-RP 1258, 1, August 1991.

8. Blandeau, V. P. and Joseph, P. F., Broadband Noise due to Rotor-Wake/Rotor Interaction in Contra-Rotating Open Rotors, *AIAA Journal*, 2010, 48(11), pp. 2674–2686.

9. Parry, A. B., Kingan, M. and Tester, B. J., Relative Importance of Open Rotor Tone and Broadband Noise Sources, in: *Proceedings of the 17th AIAA/CEAS Aeroacoustics Conference (32nd AIAA Aeroacoustics Conference*), Portland, OR, 05–08 June 2011.

10. Sree, D., Development of an Improved Data Reduction Tool for Analyzing Far-field Acoustic Data from Counter-Rotating Open Rotors, Report, *2010 Summer* NASA-GRC

Faculty Fellowship Program (NGFFP), University Affairs Office, NASA-GRC, Cleveland, OH, 10 August 2010.

11. Sutliff, D. L., Private Communications, 2012.

12. Cooper, B.A., A Large Hemi-Anechoic Chamber Enclosure for Community-Compatible Aeroacoustic Testing of Aircraft Propulsion Systems, *Journal of the Institute of Noise Control Engineering of the USA*, January–February, 1994.

WIND TURBINES LOW FREQUENCY NOISE ISSUE DISMISSED

Wind power advocates in Australia are welcoming a study by a state agency that suggests that low-frequency noise from wind farms is not significant. The South Australia Environmental Protection Agency study said the infrasound readings “at rural locations both near to and away from wind farms were no higher than infrasound levels measured at ... urban locations.” Moreover, “the results at one of the houses near a wind farm are the lowest infrasound levels measured at any of the 11 locations included in this study.” The Clean Energy Council, an Australian renewables trade group said “This is yet another clean bill of health for wind farms, which have been proven time and time again to cause no negative health impacts from noise.” In a “context” summary released after the study came out, the EPA did point out that “testing has only been undertaken at two locations adjacent to wind farms and therefore general conclusions cannot be drawn based on these data alone.”

SPECIAL NOISE REGS FOR WIND TURBINE

Massachusetts will look into drafting separate noise regulations for wind turbines, according to Department of Environmental Protection Deputy Commissioner Martin Suuberg. Speaking at a municipal wind conference at the University of Massachusetts Dartmouth, Suuberg said he had no details on the regulations yet but that “there is a different quality of noise generated by turbines. This is something we will be exploring further,” Suuberg said. Currently, industrial wind turbines fall under the same state noise regulation as all other industrial facilities. Under that regulation, a noise source is in violation if it is more than 10 decibels louder than an area’s background noise. Some SouthCoast and Cape Cod towns have already begun to explore changing their local sound regulations to only allow a six-decibel difference for turbines. Suuberg said that idea is something he would have to look into and he also said he personally has heard of turbine regulations in Europe where there is an overall cap on how loud ambient sound - with or without turbines - can go. “We recognize a need to look into this but now we have a question of what’s the right standard,” he said.

NOISE REGULATIONS HITTING LIVE MUSIC?

Dr Ianto Ware has been appointed National Live Music Coordinator by Australia's Federal Arts Minister Simon Crean. The National Live Music Coordinator's agenda focused on easing the problematic state and national regulations that restrict the development of Australia's live music scene, dealing with the number of venues closing their doors, and putting the interests of musicians first. Dr Ware stated that, over the next three years, he aims to identify ways of untangling the complex web of 'party-killing laws' – such as noise complaints, liquor licensing issues, and environmental concerns – that are damaging live music at a local level. Dr Ware said, "whilst live music is one of the most popular forms of cultural activity in the country, something like 70% of venues said regulation had a serious impact on their capacity to host it." There's an increased sense of communities having problems finding stages to perform on and maybe not getting the opportunities they deserve. So they hired somebody to work across states, look at what the problems are and what the possible solutions are," he continued. "Some local government approaches to handling the planning issues are really negative. So we're seeing fewer opportunities for people to get involved in live music: fewer opportunities to work on stages, for people to learn how to book and manage venues, or be publicists or band managers, because there's not that entry level left anymore." The National Live Music Coordinator also spoke about the problems of noise complaints by "vexatious residents," saying "noise complaints are handled differently from state to state. Often they're not handled with the welfare of small business in mind." Later noting, "one of the common things we see is that a venue was hosting live music, but they start to decrease it and stop it. And it's usually to do with noise complaints or planning issues."